OPTICAL SIGNAL PROCESSING AND TELEVISION BANDWIDTH COMPRESSION

by

THIEN-KE CHU

B.A.Sc., Universite de Montreal, 1968

A THESIS SUBMITTED IN PARTIAL FULFILMENT OF THE

REQUIREMENTS FOR THE DEGREE OF

MASTER OF APPLIED SCIENCE

in the Department of

Electrical Engineering

We accept this thesis as conforming to the

required standard

Research Supervisor .....

Members of Committee.....

.....

Acting Head of Department.....

Members of the Department of

Electrical Engineering

THE UNIVERSITY OF BRITISH COLUMBIA

September, 1970

In presenting this thesis in partial fulfilment of the requirements for an advanced degree at the University of British Columbia, I agree that the Library shall make it freely available for reference and study. I further agree that permission for extensive copying of this thesis for scholarly purposes may be granted by the Head of my Department or by his representatives. It is understood that copying or publication of this thesis for financial gain shall not be allowed without my written permission.

Department of Electrical Engineering

The University of British Columbia
Vancouver 8, Canada

Date September 29, 1970

ABSTRACT

A television band compression scheme which depends primarily on matching in one sense the eye's sensitivity to flicker has been proposed. For a static picture as the source material, it is found that the compression ratio is not directly limited by the flicker effect, but the picture quality assessed subjectively, falls quite fast as the compression ratio is increased. A compression ratio of 1.5:1 is accompanied by a very small drop in subjective quality. Using a "high frequency boost" circuit the compression ratio can be increased to 3:1 under conditions of satisfactory picture quality.

Experiments were performed using as source a movie picture, and higher compression ratios than those for the static picture were indicated.

All the experiments were performed using a simulated television transmission system. The system was based on a laser source, and it is an improvement on a system designed by Otto Meier in 1968.

TABLE OF CONTENTS

LIST OF ILLUSTRATIONS

ACKNOWLEDGEMENT

I am deeply indebted to my supervisor, Dr. M.P. Beddoes for more than just his advice and encouragement.

I am grateful to Dr. B.P. Hildebrand for reading the manuscript.

I am thankful to Dr. E.V. Bohn for giving the very accurate motor; Mr. W. Walters and Mr. Chris Sheffield for their help in selecting the accessories; Mr. C.G. Chubb and Derek Daines for building the equipment; Mr. Herb Black for valuable photographic work. I express my sincere appreciation to Miss Veronica Komczynski for typing the manuscript; Mr. G.J. Fitzpatrick and Mr. J. Bennett for proofreading.

Finally I also wish to express my thanks to the National Research Council of Canada for financial assistance.

I. INTRODUCTION

Numerous publications and references [1] - [5], [11] deal with the television bandwidth compression problem. The need for visual communication is increased every day and a plethora of devices have been proposed in this field. An example is the visual telephone. It is said [4] that the sending of banking messages and the exchanging of technical drawing messages will only be possible if a new television system using relatively narrow bandwidth can be made available.

Compression techniques have been classified [5] into three different categories: pure statistical, psychophysical and a combination of the two. An example of the pure statistical approach is the work done by Colin Cherry et al. [4]. They pioneered a run-length-coding method and compression ratios of up to 3.5:1 for a half tone picture have been obtained. Very elaborate work has been done by Schreiber's group [3] in which the combination approach has been used. They took advantage of the fact that the eye is very sensitive to the detection of edges and they proposed a system called "Synthetic Highs". Experiments were carried out by computer-simulation and efficient coding and quantizing methods were investigated. The results were good, as shown by high compression ratios of 5 or 6 to 1 for a half tone picture [5]. In comparison with building electronic equipment, computer-simulation has many advantages. However, computer simulation cannot be used for real time studies because it takes many seconds to generate a single picture frame, and it is virtually impossible to study the real television situation which involves motion pictures.

An experimental system based on a coherent light source for processing visual signals has the remarkable property that it is very fast.

Real time studies can be undertaken and these can include the motion picture problem. This analog system has noise problems but these can be tolerated by the eye and filtering is easy to realize. In particular we have used such an optical system to perform the Fourier and the inverse transform; we could therefore study bandwidth compression under conditions which approach the practical case very closely.

A start to the work reported here was made in 1968 by Otto Meier [1], [2]. In his work a series of high quality and low quality versions of the same picture were presented alternately for equal intervals of time, T, on a television monitor and a viewer was asked to state if he could see any flickering in the display. Meier showed that the eye is sensitive to flicker frequency by very different amounts according to the highest spatial frequency present in the picture. With a view to obtaining reduction in channel bandwidth, it seemed natural to suggest that the television picture source encoder could be designed to match more closely the flicker sensitivity of the eye. Although one can predict that up to 2:1 compression should be possible from Meier's results, he did not explore higher potential compression ratios.

In the present work the apparatus used by Meier has been improved so that higher quality resolution was obtained. This enables us to explore further the proposed compression scheme. The absence of flicker is only one criterion that the compression scheme must meet. One might ask how much the subjective impression of picture quality falls as the compression ratio, C, is increased. A further series of tests were made using a series of graded photographs in which a subject was asked to pair pictures having similar subjective picture quality. Using this technique, it was found that the picture quality falls quite fast as C is increased, but a "high frequency boost" circuit offsets to a certain degree this decline.

II. BASIC OPTICAL SYSTEM AND CALCULATION

Meier's optical processing system used a laser, three lenses and a closed circuit television camera-monitor display. A solution to the problem of placing the lenses was arrived at using trial and error techniques. An adequate theory to give the positions of the lenses and the stop sizes was not available. This deficiency is supplied by the theory part given in this chapter which is based on Vander Lugt's notation [6].

2.1 Basic Optical Elements

2.1.1 Spatial Fourier Transform

A spatial Fourier transform of a pattern is an array of points whose position corresponds to frequency, and brightness corresponds to amplitude. Fig. 2.1 shows a simple test pattern and its one- and two-dimensional Fourier transform. Fig. 2.2 shows a half-tone picture and its Fourier transform.

2.1.2 Approximation and Operational Notation of Some Basic Elements

(a) light wave and film

light wave: $A(x,y) = |A(x,y)|\exp[j\phi(x,y)]$

film: $f(x,y) = |f(x,y)|\exp[j\theta(x,y)]$

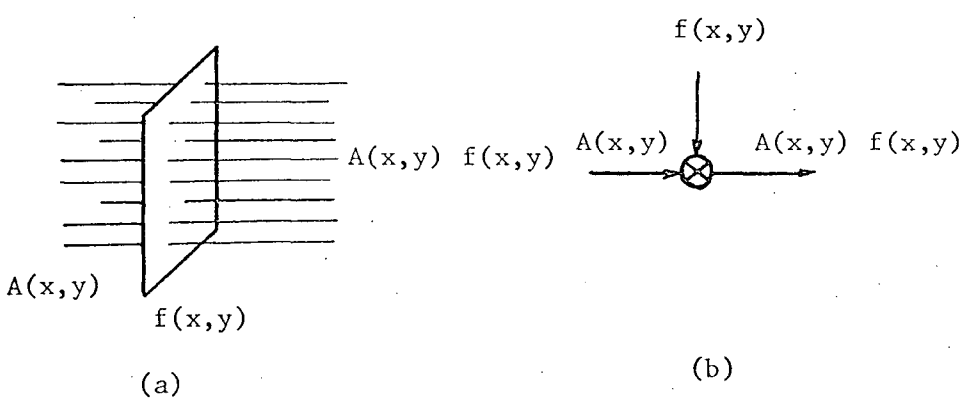

Fig. 2.3 Light Wave and Film
(a) Optical System
(b) Block Diagram

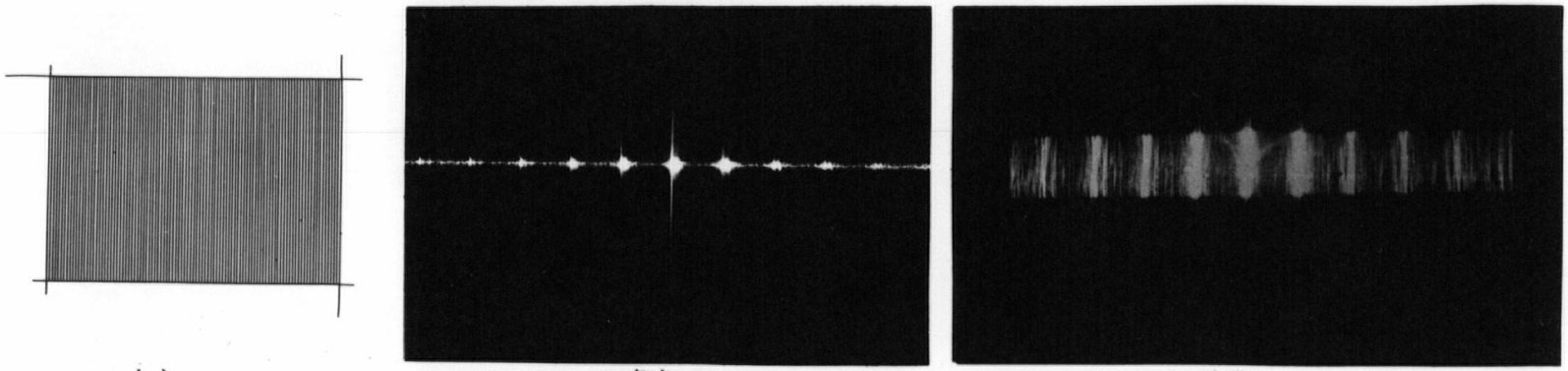

(a) (b) (c)

Fig. 2.1 (a) Lines test pattern (b) Two-dimensional Fourier transform of (a) (c) One-dimensional Fourier transform of (a)

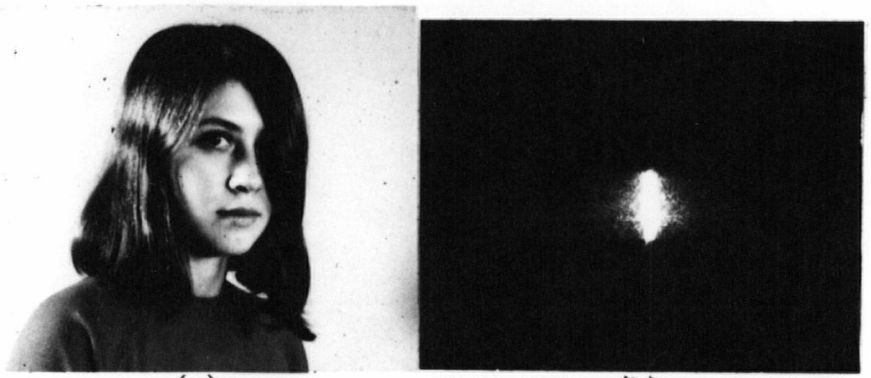

(a) (b)

Fig. 2.2 (a) Half-tone picture (b) One-dimensional Fourier transform of (a)

(b) Spherical lens

If F = Focal length; $f = \frac{1}{F}$ and a function ψ is defined as follows:

$$\psi(x,y;f) = \exp\left[j \frac{kf}{2}(x^2 + y^2)\right]$$

Then the approximation and notation of a spherical lens will be:

$$\bar{\psi}(x,y;f) \equiv \exp\left[-j \frac{k}{2F}(x^2 + y^2)\right]$$

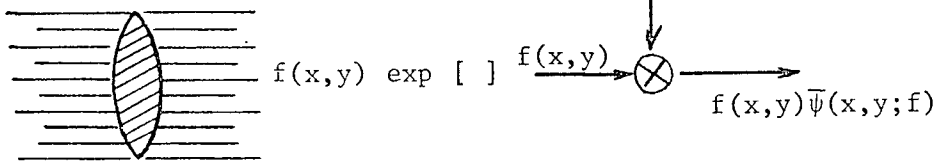

f(x,y) $\exp\left[-j \frac{k}{2F}(x^2 + y^2)\right]$

(a) (b)

Fig. 2.4 Spherical Lens
(a) Optical System
(b) Block diagram

(c) Cylindrical lens

$$\bar{\psi}(x;f) \equiv \exp\left[-j \frac{k}{2F} x^2\right]$$

$$\bar{\psi}(y;f) \equiv \exp\left[-j \frac{k}{2F} y^2\right]$$

(d) free space

D = distance between two planes

$$d = \frac{1}{D}$$

approximation of free space will be:

$$d \cdot \psi(x,y;d) \equiv \frac{1}{D} \exp\left[j \frac{k}{2D}(x^2 + y^2)\right]$$

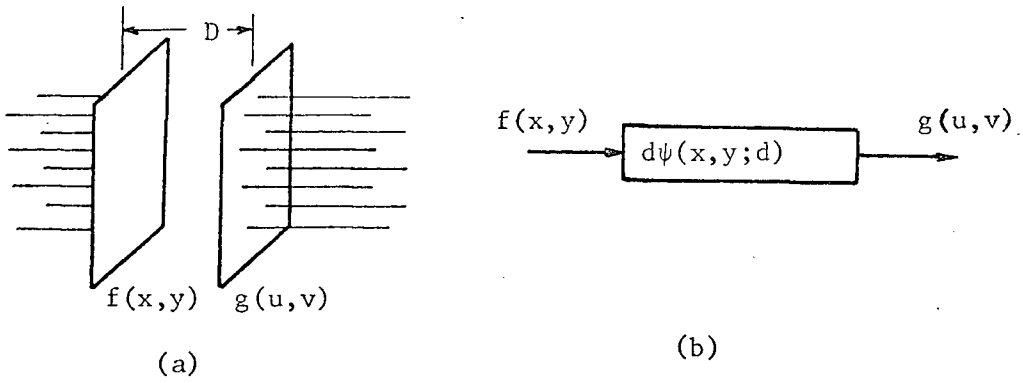

Fig. 2.5 Free space

(a) Optical System

(b) Block Diagram

2.2 Design of the Optical System

The system using optical filtering techniques for this work consists of three parts (Figure 2.6). The first part displays a Fourier transform F(u,v) of a spatial pattern f(x,y), in plane P_2. The second part is a filter H(u,v)-a side band stop and a chopping wheel-in plane P_2. The last part gives the inverse Fourier transform of the product F(u,v)·H(u,v). Such a system is described by Vander Lugt [6] as a Variable-Scale Correlator.

The necessary modification is made, two cylindrical lenses are inserted in their appropriate places to obtain a "one-dimensional" Fourier transform and reconstruction.

To simplify the calculation, we assume that $L_1 = 0$; $L_4 = 0$. Such an approximation is very reasonable because of two reasons:

1. All lenses are weak, that means: $F_1, F_2, F_3, L_2, L_3, L_5, L_6 >>> L_1, L_4$

2. The lenses are not perfect; after some accurate calculation fine adjustment by trial and error should be made.

The set up in this lab. is a 1:1 symmetrical system. The symmetrical system is simpler than one with a scale change. Meier [2] remarks that it is practically impossible to align the asymmetrical system.

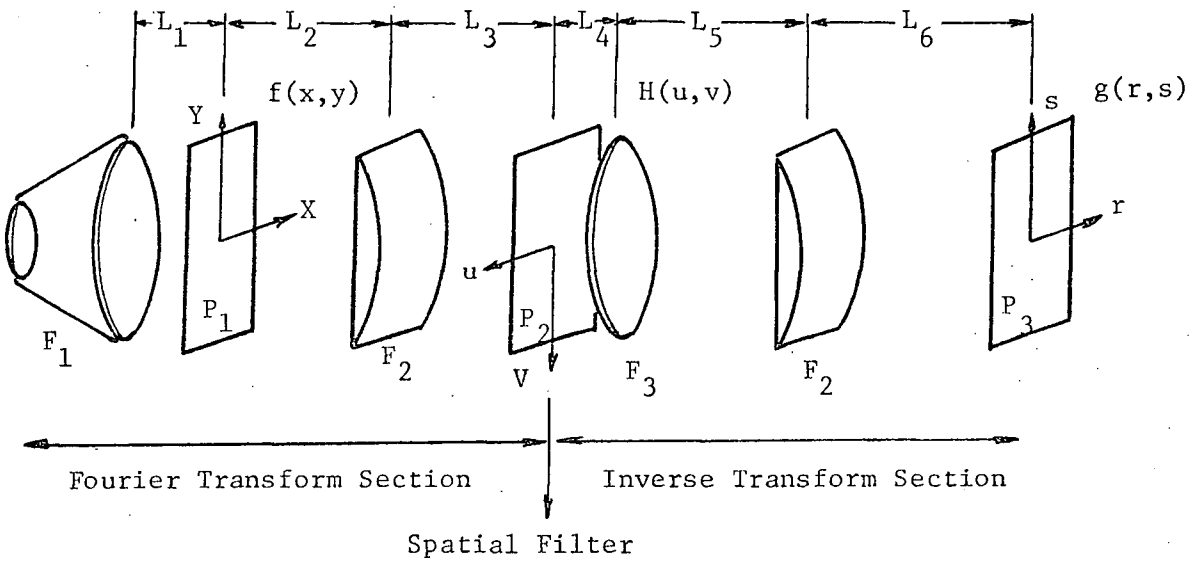

Fig. 2.6 The Optical System Experimented

F_1: Laser beam expander

F_2: Cylindrical lens

F_3: Spherical lens

P_1: Input plane

P_2: Fourier Transform plane

P_3: Output plane

To attain the one to one symmetrical set up the separations in Fig. 2.6 should satisfy the following equalities.

$$L_3 = L_5 \tag{2.1}$$

$$L_2 + L_3 = L_5 + L_6 = 2F_3 \tag{2.2}$$

If a two dimensional spatial coordinate test pattern function $f(x,y)$ is placed in plane P_1, the light distribution in plane P_2 then will be given by equation 2.3.

$$F(u,v) = C\cdot\psi(u,v;l_3)\iint_{P_1} f(x,y)\psi(x,y;l_2-f_1)\cdot\bar{\psi}\left[x+\frac{l_3}{l_2}u;\frac{l_2^2}{l_2+l_3}\right]\cdot\bar{\psi}\left[y+\frac{l_3}{l_2}v;\frac{l_2^2}{l_2+l_3-f_2}\right]dxdy \tag{2.3}$$

To obtain the Fourier transform along the horizontal axis and image along the vertical axis in the plane P_2, the conditions for setting lenses are as follows:

Imaging condition on vertical axis

$$\frac{l_2^2}{l_2 + l_3 - f_2} \longrightarrow \infty \tag{2.4}$$

or

$$\frac{1}{L_2} + \frac{1}{L_3} = \frac{1}{F_2} \tag{2.5}$$

Fourier transform condition

$$l_2 - f_1 - \frac{l_2^2}{l_2 + l_3} = 0 \tag{2.6}$$

or

$$F_1 = L_2 + L_3 \tag{2.7}$$

The proof of equations 2.3, 2.5, and 2.7 will be found in Appendix A-2.

The lenses used here have the following characters.

Laser beam expander	F_1 = 4 meters
Spherical lens	F_3 = 2 meters
Cylindrical lenses	F_2 = 0.8 meter

In solving equations 2.5, 2.7, 2.1 and 2.2 the axial positions of lenses are obtained as in Table 1.

TABLE 1

	Theoretical	Experimental	Error
L_2	2.895m	2.90	0.2%
L_6	2.895m	2.91	0.5%
L_3	1.105m	1.1	0.5%
L_5	1.105m	1.09	1.4%

The close correspondence between experimental and theoretical values in Table 1 indicates that the first order theory used in this theoretical treatment is quite adequate.

2.3 Frequency and Image-Position Relation

In this one to one system a 16 mm width picture in the input plane will correspond to a 16 mm width picture in the output plane which is received by a vidicon. The finest resolution can be resolved by the vidicon is 250 lines/picture width, in this case 250 lines/16 mm.

To relate the position of image points in the F.T plane to frequency, f_x, in lines/p.w. in the input and the output planes a simple test pattern was used. The distance from the first to second maxima was measured and it is proportional to the number of lines/p.w. in the input and the output pictures.

The calibration is shown in Fig. 2.7 and it demonstrates that $f_x \alpha x$ - a linear dependence -.

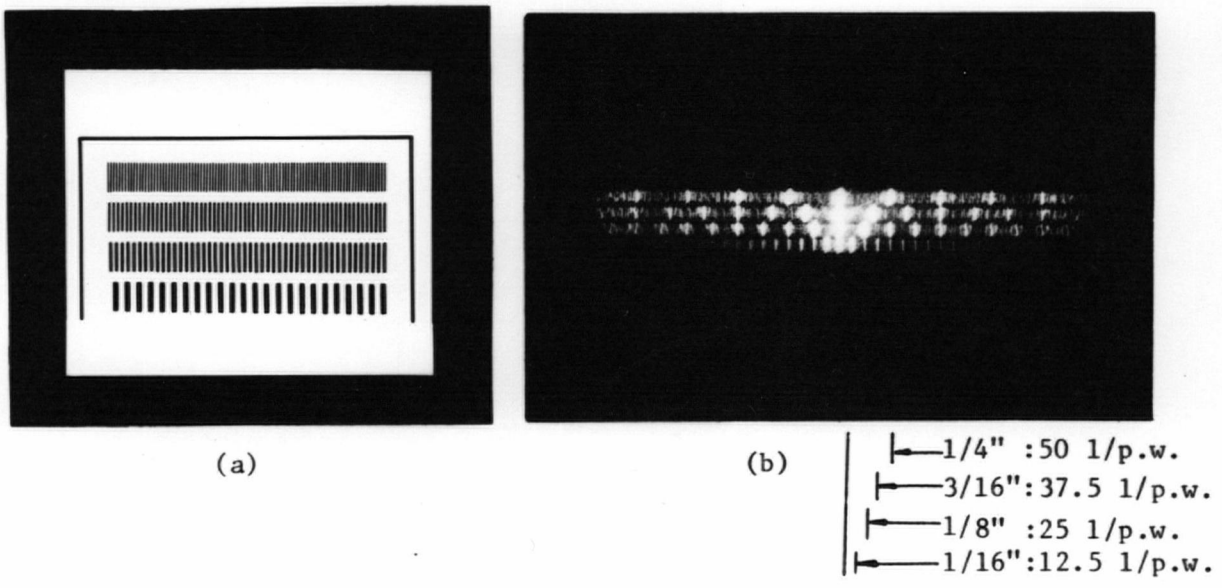

Fig. 2.7 Image-Position Relation in Fourier Transform Plane

(a) enlarged photo of a test pattern
(b) one dimensional F.T of (a) shows a linear dependence of fx with respect to x

III. STATIC PICTURE TESTS

In this chapter a brief description of test procedure, apparatus and results are given. It contains results of flicker experiments in which the high quality picture is presented for a period T_H and the low quality picture for T_L and it is shown that the sensation of flicker is largely independent of $\frac{T_L}{T_H}$. This suggests that large compression ratios might be possible. The subjective evaluation of compressed pictures was also measured and related to band-reduced but otherwise normal television pictures. It is shown that picture quality falls rapidly as the compression ratio is increased but it is also shown that a high frequency boost circuit arrests to a certain limit this deterioration.

3.1 Basic Idea

The compression scheme considered here presents a series of high quality and low quality versions of the same picture. The high quality picture contains dc up to a highest spatial frequency fm. The low quality picture contains dc up to a spatial frequency fx. The difference between the two sets of pictures is due to the spatial frequency components lying between fx and fm and it will be shown that the eye needs to have these components replenished at a low rate. Thus the basic idea is to produce such pictures by a two-velocity-scanning system and this will result in a reduction in the channel bandwidth.

The experiments reported were performed using the analog apparatus described in the next section.

Define:

T_L: period in which low quality video signal is sent

T_H: period in which high quality video signal is sent

fm: highest spatial frequency in high quality picture (lines/ picture width)

fx: highest spatial frequency in low quality picture (lines/ picture width)

f: frame repetition frequency

F: the bandwidth needed to pass the high quality picture (in Hz)

F_R: the bandwidth of the compressed system

S: dimension proportional constant (lines/p.w. and Hz)

If
$$\frac{T_L}{T_H} = R \tag{3.1}$$

$$F = S \cdot 60 \cdot fm$$

$$F_R = S \cdot f \cdot [\frac{R\ fx + fm}{1 + R}]$$

$$F_R = F \cdot \frac{f}{60} [\frac{1 + R \cdot fx/fm}{1 + R}] \tag{3.2}$$

The experiments obtained the limit $fc \leq f/(1+R)$ for which the flicker effect is just not noticeable under a number of conditions.

$$fc = f(R, fx, \text{Contrast}, \text{Brightness}) \tag{3.3}$$

$$fc = \frac{1}{T_H + T_L} = \frac{1}{T_H(1+R)} \tag{3.4}$$

For a fixed value T_H, $fc = F(R) = F(fx)$

$$\text{or} \qquad R = F(fx) = F(fc) \tag{3.5}$$

Thus (3.5) and (3.2) can be solved to obtain the compressed bandwidth.

3.2 Test Arrangement

Different pictures were put in the plane P_1 of Fig. 2.6 as test patterns.

A mask is placed at the Fourier transform plane P_2 to remove a

half of the spatial frequencies of a symmetrical spectrum. The total information to be reconstructed now corresponds to a single sideband of a television transmission system.

A chopping wheel with variable OFF:ON ratio, R, was used to cut all spatial frequencies above a certain limit fx temporarily at a variable repetition rate f_p. The high quality picture corresponds to the "ON" part; the low quality picture corresponds to the "OFF" part. The output picture at the plane P_3 was received directly by a vidicon (T.V. camera without lenses) and appeared on a T.V. monitor.

An experiment was started by setting fx to a chosen value and rotating the wheel, Figure 3.1. At first when the chopping wheel rotated slowly the flicker effect was very pronounced and easily observed by a subject who was at 1.5 m from the monitor. The wheel velocity was then increased to a point where the subject felt that no flickering effect appeared. The value of repetition rate at this point was recorded as fc (critical flickering frequency).

Constrast ratio and brightness can be adjusted easily on the monitor to give a pleasing picture and "maximum details". Fig. 3.2 and 3.3 show the apparatus set up.

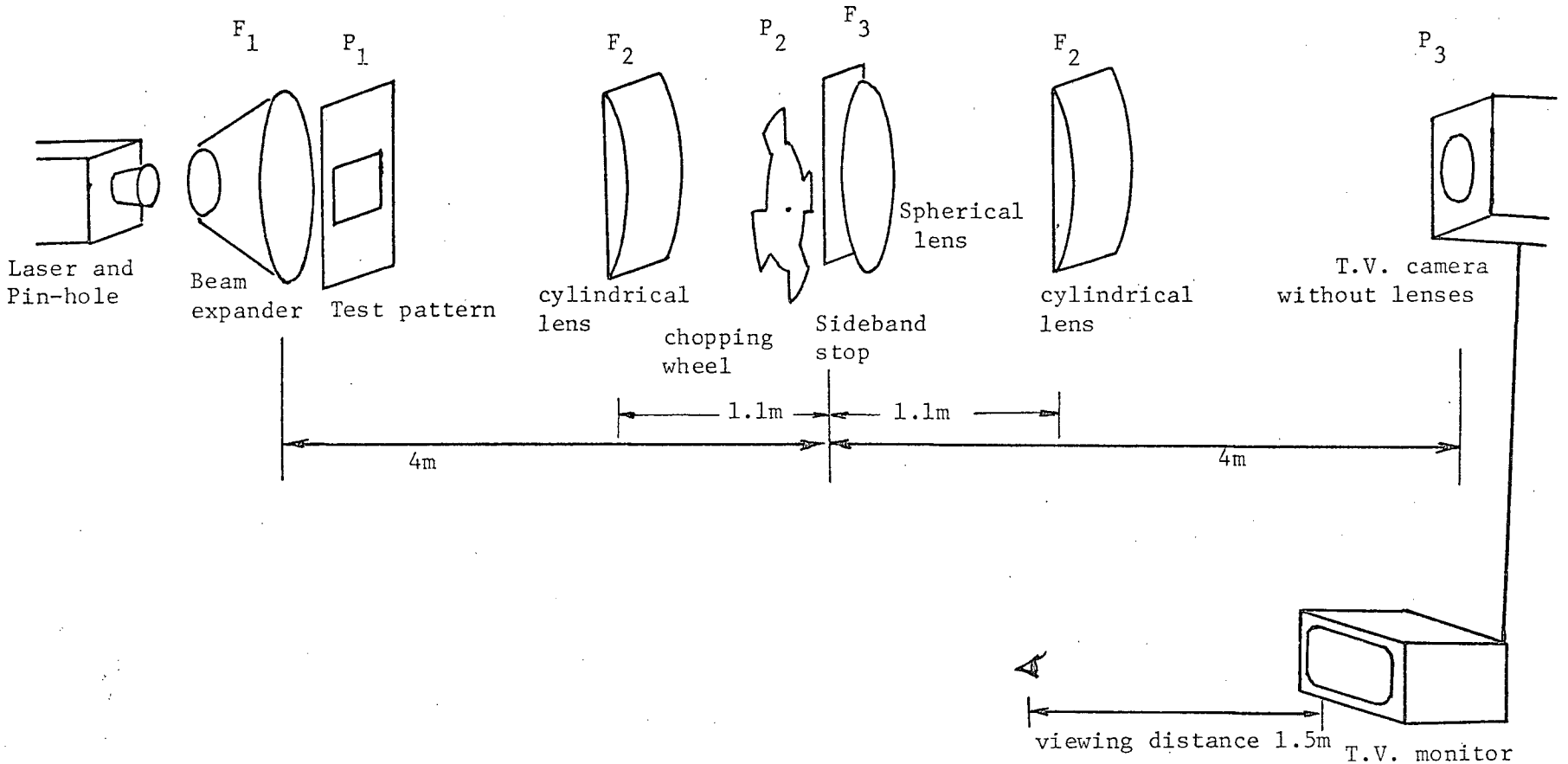

Fig. 3.1 Test arrangement

F_1: Beam expander telescope adjusted to F=4m

P_1: Input plane; Test pattern: 16 mm width slide

F_2: Cylindrical lenses; F=0.8m

P_2: Fourier transform plane; chopping wheel and sideband stop

F_3: Spherical lens; F=2m

P_3: Output plane; T.V. camera without lenses

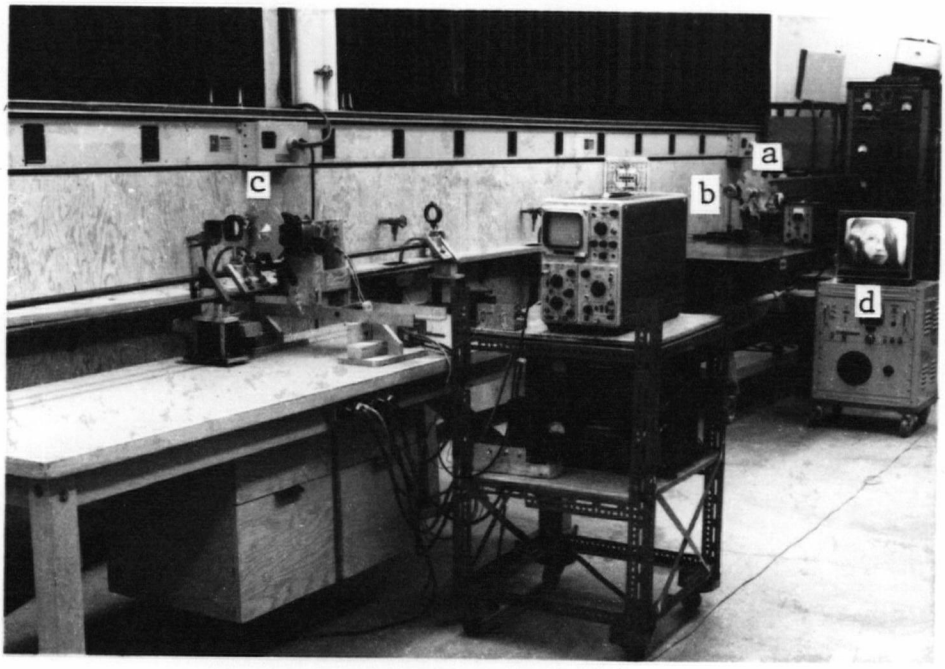

Fig. 3.2 Test Apparatus

(a) Laser and beam expander
(b) Test pattern
(c) Optical System
(d) Monitor

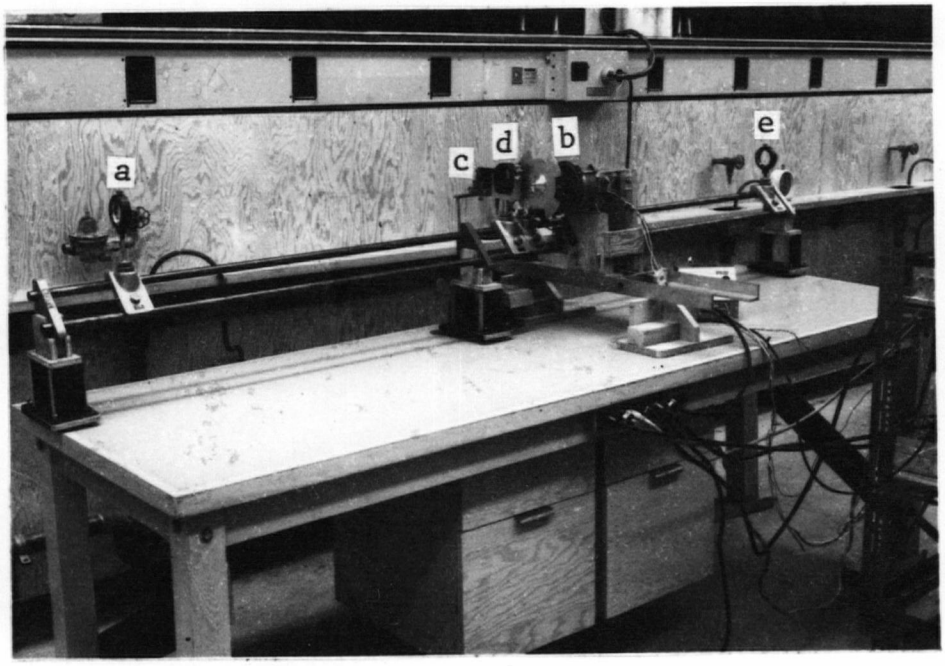

Fig. 3.3 Optical System Set up

(a)-(e) Cylindrical lenses F_2
(b) Chopping wheel
(c) Sideband stop
(d) Spherical lens

3.3 Test Results

3.3.1 Test Results

Using different test patterns and different OFF:ON ratio R = 1, 2, 3, results were obtained and they are reported on the following pages.

To check the consistency of the results, three sets of tests were carried out at different times at least one day apart.

It is shown that the experimental points varied slightly for one subject but more noticeably from one subject to another. Only the upper bound or the worse cases are presented and used for compression ratio calculations.

3.3.2 Discussion

The results of these tests show that fc is largely independent of OFF:ON ratio R. The only changing factor when R is changed, is the quality of the output picture; this point will be considered more carefully later.

The experimental points varied widely from one test picture to the other; that means fc is strongly dependent upon picture content.

Contrast ratio and brightness, as reported in Meier's thesis [2], have little influence on fc.

The mask used to suppress one sideband produced deleterious effects which are illustrated in the next section. It must be pointed out that with normal television transmission the filters which eliminate one sideband are designed to alternate at 6 db/oct on the skirts. The effects of overshoot which we experienced are much exaggerated because we used a "brick wall" filter. The problem was mitigated by placing the stop slightly off center. Computations of fx take this into account.

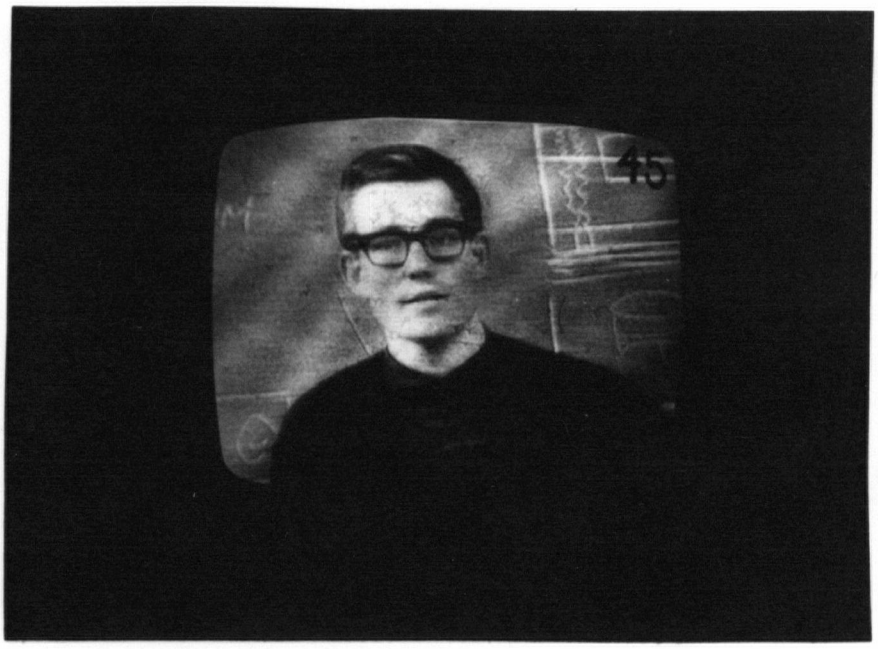

Fig. 3.4 Test Pattern No. 1

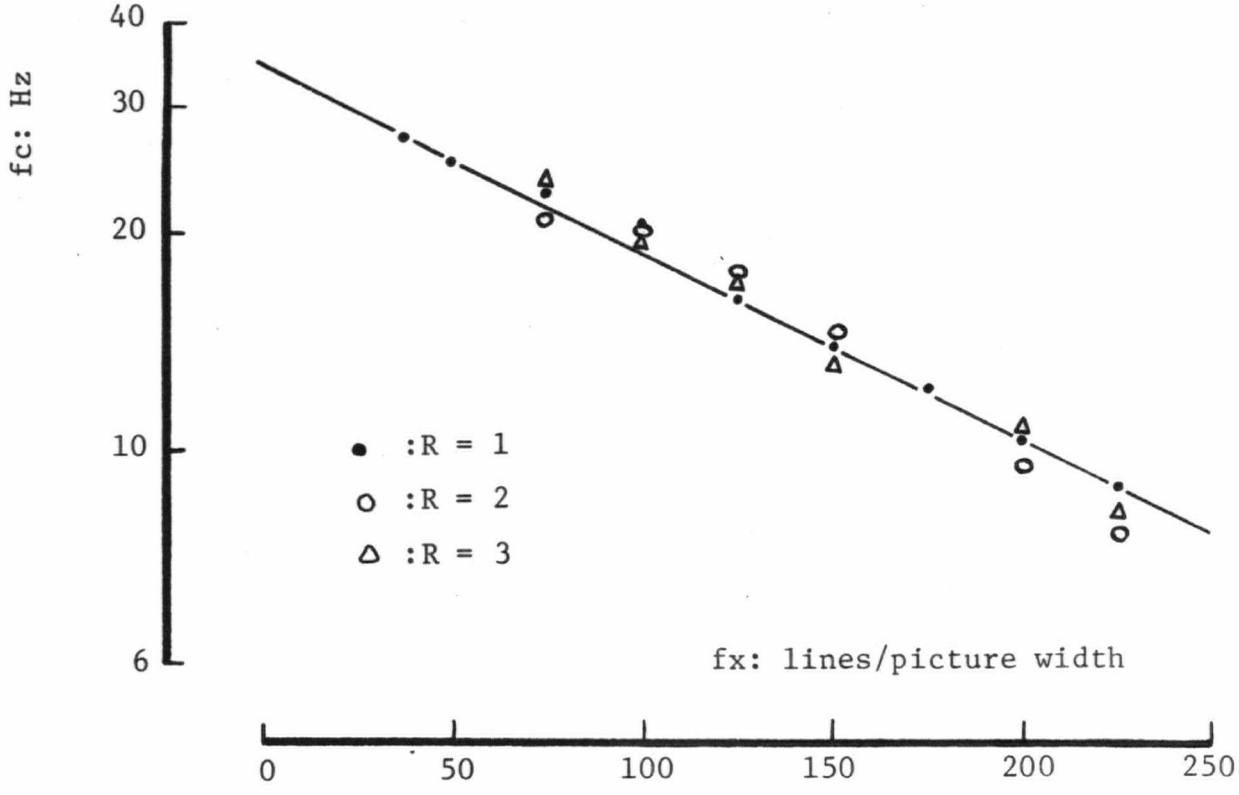

Fig. 3.5 Critical frequency as a function of limit fx of test pattern No. 1

Fig. 3.6 Test Pattern No. 2

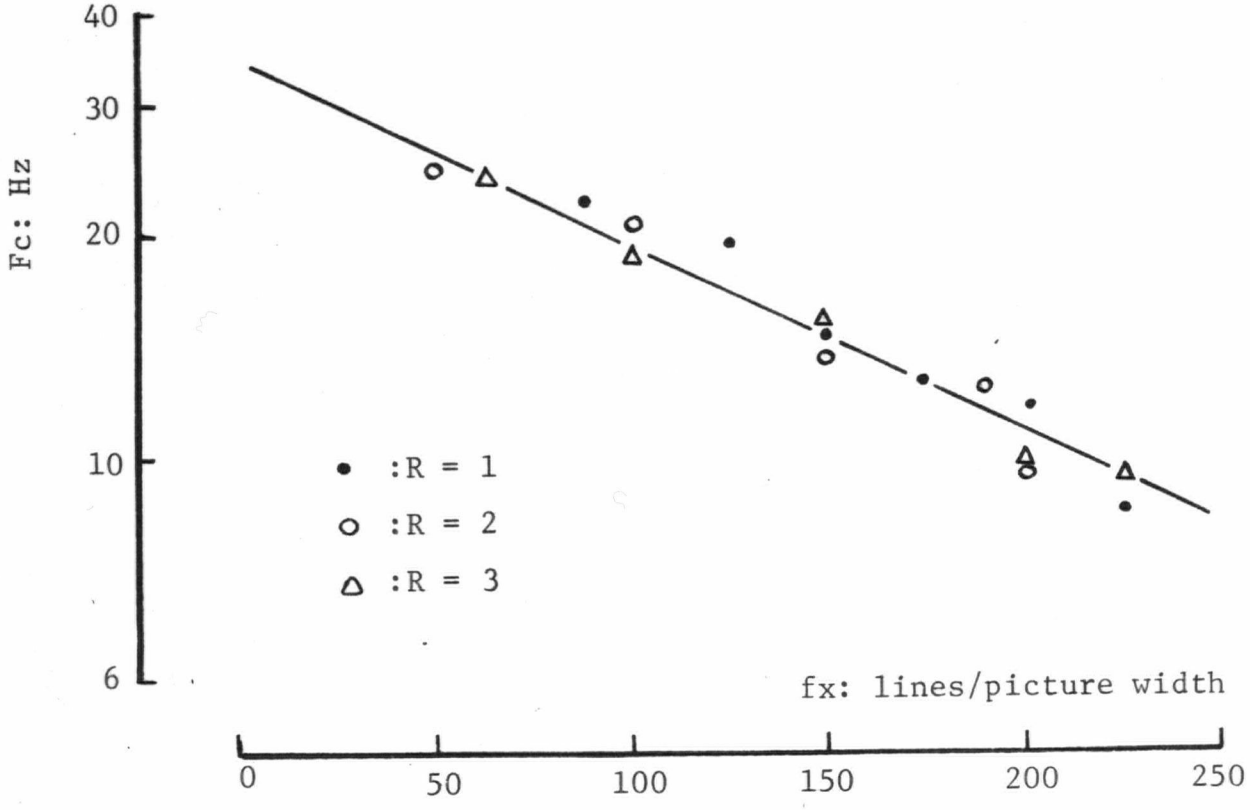

Fig. 3.7 Critical frequency as a function of limit fx of test pattern No. 2

Fig. 3.8 Test Pattern No. 3

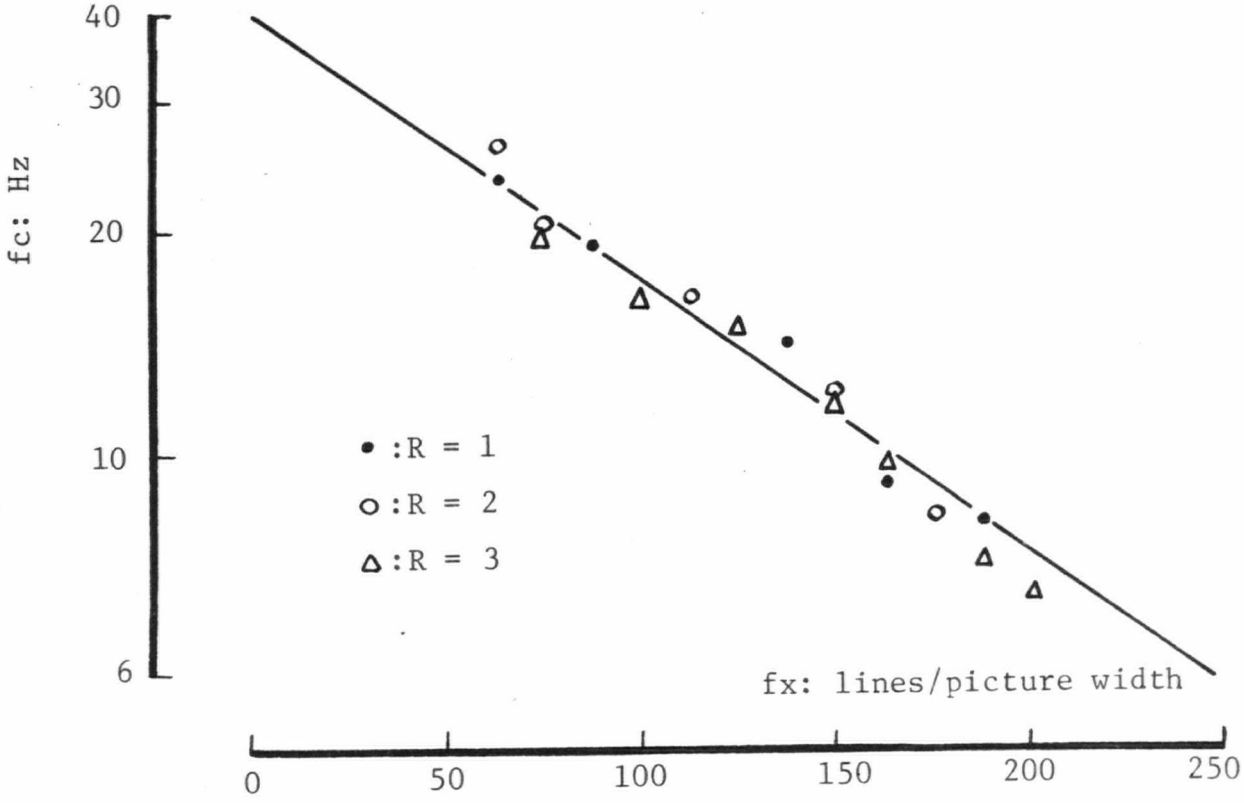

Fig. 3.9 Critical frequency as a function of limit fx of test pattern No. 3

"Over all" flickering always occurred when fx was lower than 25 lines/p.w. The value of fc at fx = 0 is just a mathematical extrapolation. The overall flickering effect is due to diffraction phenomena and will be referred to when we discuss the limitations of the system.

The expression fc = fo exp [-kfx] used to approximate the Meier's results is once again found to fit the experimental points.

Values of fo in the actual tests varied from 35 to 40 Hz. The factor k lies between 0.005 to 0.01; fc is in Hertz and fx is in lines/picture width. For the test pattern in Fig. 3.4, fc = 35 exp (-0.0056 fx); in Fig. 3.6, fc = 35 exp (-0.0055 fx); in Fig. 3.8, fc = 40 exp (-0.0095 fx).

3.4 Limitation of the Experimental System

3.4.1 Noise due to coherent light source [10]

Let g(x,t) be the complex amplitude of an optical field. The instantaneous intensity I(x,t) is given by:

$$I(x,t) = g(x,t) \cdot g^*(x,t) \tag{3.6}$$

where g*(x,t) denotes the complex conjugate.

As an image is a combination of weighted and displaced delta functions, we first examine the results of a two-point-source addition.

If $$g(x,t) = g_1(x,t) + g_2(x,t) \tag{3.7}$$

Then $$I(x,t) = g(x,t) \cdot g^*(x,t)$$

$$= g_1(x,t) \cdot g_1^*(x,t) + g_2(x,t) \cdot g_2^*(x,t) + g_1(x,t) \cdot g_2^*(x,t) + g_1^*(x,t) \cdot g_2(x,t) \tag{3.8}$$

The time average is:

$$I(x) = \lim_{T \to \infty} \frac{1}{2T} \int_{-T}^{T} I(x,t)\,dt \tag{3.9}$$

Incoherent addition

In the incoherent case $g_1(x,t)$ and $g_2(x,t)$ both vary randomly with time and also vary randomly with respect to each other.

$$\lim_{T\to\infty} \frac{1}{2T} \int_{-T}^{T} g_1(x,t)\cdot g_2^*(x,t)dt = \lim_{T\to\infty} \frac{1}{2T} \int_{-T}^{T} g_1^*(x,t)\cdot g_2(x,t)dt=0 \tag{3.10}$$

$$I(x) = I_1(x) + I_2(x) \tag{3.11}$$

in general for n points

$$I_n(x) = \sum_{i=1}^{n} I_i(x) \tag{3.12}$$

Coherent addition

For coherent light:

$$g(x,t) = g_1(x,t) \pm g_2(x,t) = g_1(x)e^{-j2\pi\nu t} + g_2(x)e^{-j2\pi\nu t} \tag{3.13}$$

where

$$g_1(x) = A_1(x)e^{j\phi_1(x)} \tag{3.14}$$

$$g_2(x) = A_2(x)e^{j\phi_2(x)} \tag{3.15}$$

Then

$$I(x) = |A_1(x)|^2 + |A_2(x)|^2 + A_1(x)\cdot A_2(x)\{e^{j[\phi_1(x)-\phi_2(x)]} + e^{j[\phi_2(x)-\phi_1(x)]}\} \tag{3.16}$$

or

$$I(x) = |g_1(x) + g_2(x)|^2 \tag{3.17}$$

In general:

$$I_n(x) = \left|\sum_{i=1}^{n} g_i(x)\right|^2 \tag{3.18}$$

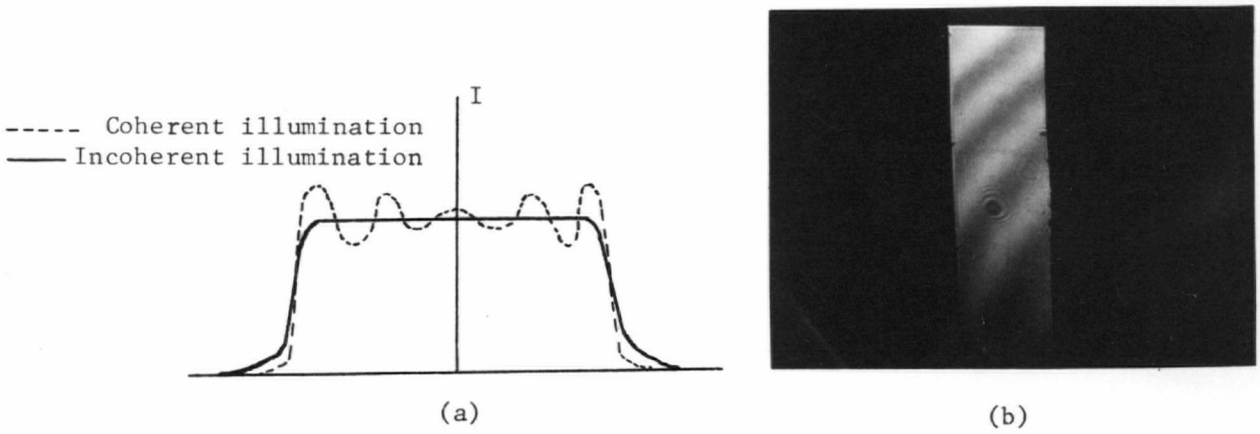

Fig. 3.10 (a) Theoretical intensity distribution in the coherent and incoherent image of a bar test (after Skinner [10])

(b) Photograph from T.V. monitor

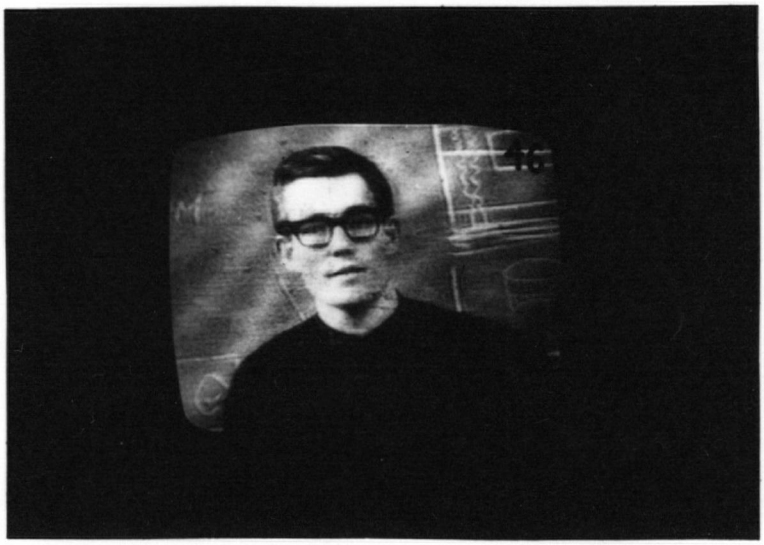

Fig. 3.11 "Contour noise" effects on a half-tone picture due to coherent illumination

The effect of these cross-correlation terms in case of a bar test pattern is shown theoretically and experimentally in Fig. 3.10. Fig. 3.11 shows this effect on a half tone picture.

The fringes due to coherent illumination are the main contributors to the flickering effect for high values of fx. Flicker was perceived by the variation in intensity of fringe lines rather than the variation of edges in the picture.

3.4.2 Limitation of fx in low frequency range

As mentioned earlier, when the chopping wheel went too close to the sideband stop, (fx < 25 lines/p.w.) the flickering of the total area occurred. This fact can be explained by examining the Fourier transform of a bar test pattern. Fig. 3.12(b) shows the intensity distribution in Fourier transform plane of a bar test pattern. The width L of the 0^{th} order diffraction pattern varies depending upon the size W of the bar test. In Fig. 3.12 $L \simeq 30$ lines when $W \simeq 1/18$ of picture width. If the wheel is in the position shown in Fig. 3.12(b) then the output light from plane P_2 (Fig. 2.6) will act like a single slit light source. Reconstruction lenses will produce a series of fringes in output plane P_3. These fringes are the cause of overall flickering and are shown in Fig. 3.12(c).

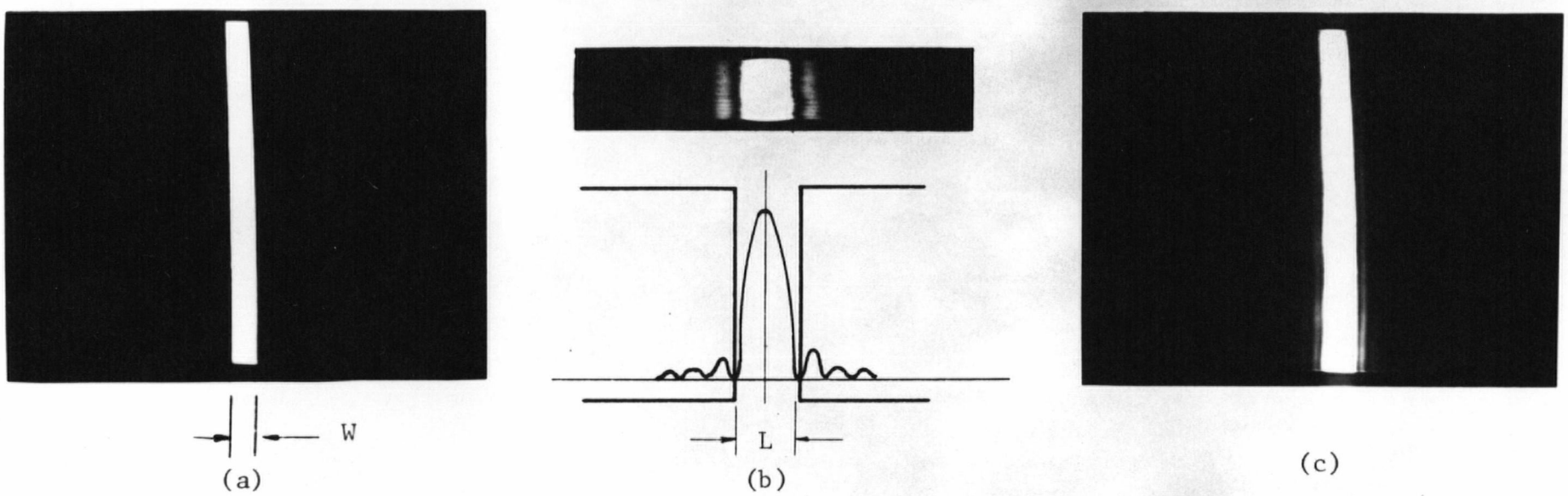

Fig. 3.12 (a) Output of a bar test pattern from T.V. monitor fx = fm
(b) Spatial one-dimensional Fourier transform of (a)
(c) Fringes due to limitation of bandwidth fx<20 lines/p.w., output from T.V. monitor

3.5 Bandwidth Compression Ratio Calculations

For realizing the television system we propose a method using two scanning velocities, a slow one for high quality pictures and a fast one for band limited pictures.

Equation 3.2 can be used to calculate the compression ratio C, for such a system.

$$F_R = F \frac{f}{60} \left[\frac{1 + Rfx/fm}{1 + R} \right]$$

$$C = \frac{F}{F_R} = \frac{60}{f} \left[\frac{1 + R}{1 + Rfx/fm} \right] \tag{3.19}$$

In the limit case $f = (1 + R)fc \leq 60$

$$C = \frac{60}{fc} \left[\frac{1}{1 + Rfx/fm} \right] \tag{3.20}$$

If we fix $T_H = \frac{1}{60}$ second

then

$$fc = \frac{60}{1 + R} \tag{3.21}$$

for each value of R, fc can be calculated, and the corresponding limit fx can be found in the curves fc vs. limit fx.

Example: calculating the maximum compression ratio for test pattern No. 2, Fig. 3.6.

1. R = 1

$$fc = \frac{60}{1 + R} = 30$$

fig. 3.7 gives fx $\simeq$ 30 lines/p.w.

$$C = \frac{60}{30} \left[\frac{1}{1 + 30/250} \right] \simeq 1.8$$

2. R = 4

$$fc = \frac{60}{1 + R} = 12$$

fig. 3.7 gives fx — 180 lines/p.w.

$$C = \frac{60}{12} \left[\frac{1}{1 + 4 \times 180/250} \right] \simeq 1.29$$

It is interesting to note that the compression ratio in this case goes down when the OFF:ON ratio is increased.

The upper limit of 1.8 for compression is disappointing but this is predicated on the method of keeping T_H equal to a whole frame period. This will not allow us to compress by a large amount. Other questions are: What is the resulting picture if we send only one part of the high quality picture instead of a whole frame? How does the degradation change with respect to the compression ratio? The work following provides answers to these questions.

3.6 Picture Quality Studies

3.6.1 Potential compression ratio

High quality picture period in this case is:

$$T_H = \frac{1}{(1+R)fc} \neq 60$$

The compressed bandwidth then is:

$$F_R = S \cdot \frac{60}{(1+R)fc} \cdot fc[Rfx + fm]$$

$$F_R = \frac{S \cdot 60}{(1+R)} \cdot [Rfx + fm] \qquad (3.22)$$

The compression ratio will be:

$$C = \frac{F}{F_R} = \frac{S \cdot 60 \cdot fm}{\frac{S.60}{(1+R)}[Rfx + fm]}$$

$$C = \frac{1 + R}{1 + Rfx/fm} \qquad (3.23)$$

C tends to (1 + R) when fx goes to zero.

The relation between compression ratio and quality of the resulting picture will be found in the next section.

3.6.2 Test results showing degradation vs. C

In order to gain high compression ratios we must take advantage of the eye, by sending fc sets of fraction- of -picture-frames instead of fc sets of whole frames. However for C large the difference in quality is pronounced and noticeable. In this section the relation between compression ratio and picture quality is reported.

To perform the test two series of pictures were taken. One of them is a series of bandlimited but otherwise normal pictures; the others are pictures obtained by varying OFF:ON ratio R and fc. The assumption is made that the picture seen by the camera and by the eye are the same. In order to check the assumption, a long exposure time was set, and a printed picture obtained; this was compared with respect to certain critical detail, with the same picture at a back of an unloaded camera. A close similarity was established.

The subjects were asked to match the compressed pictures to band-limited pictures. The quality of the picture was divided according to the highest frequency contained in the bandlimited pictures.

Two criteria were used to judge the picture quality in this test.

(1) Details of the picture; this is related to high frequency range.

(2) Overall pleasantness of the picture; this seems to be related to low frequencies range and the noise.

The results are summarized in Fig. 3.13.

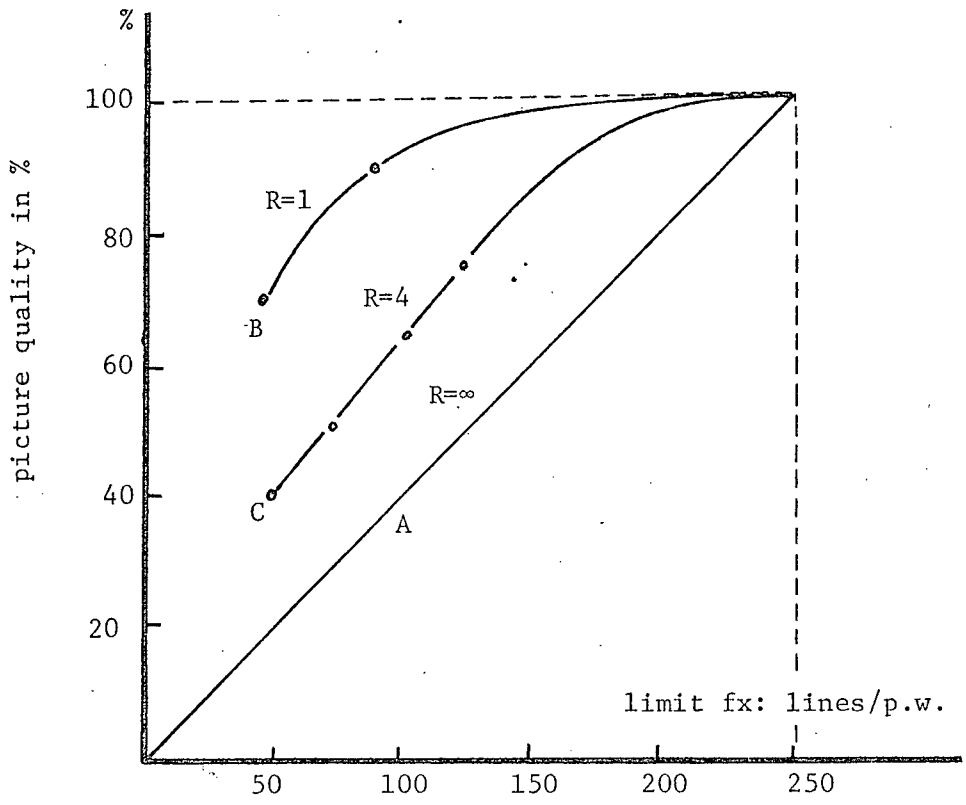

Fig. 3.13 Results of picture-quality-tests

A. Band limited pictures
B. Compressed pictures; R=1
C. Compressed pictures; R= 4

Applying equation 3.23 to the experimental points of Fig. 3.13 we obtain the compression ratios for different resulting output pictures. The results are presented in Fig. 3.14; picture quality vs. compression ratio.

3.6.3 Discussion

Before discussing the results of this test, a few things related to the picture quality should be mentioned.

From Fig. 3.15 to 3.18 we see that the quality of the pictures decreases noticeably. Fig. 3.16, 3.17 and 3.18 have the same bandwidth but different output from the Fourier transform plane. Fig. 3.16 corresponds to a double sideband modulation in plan P_2 with fx = fm; the quality of

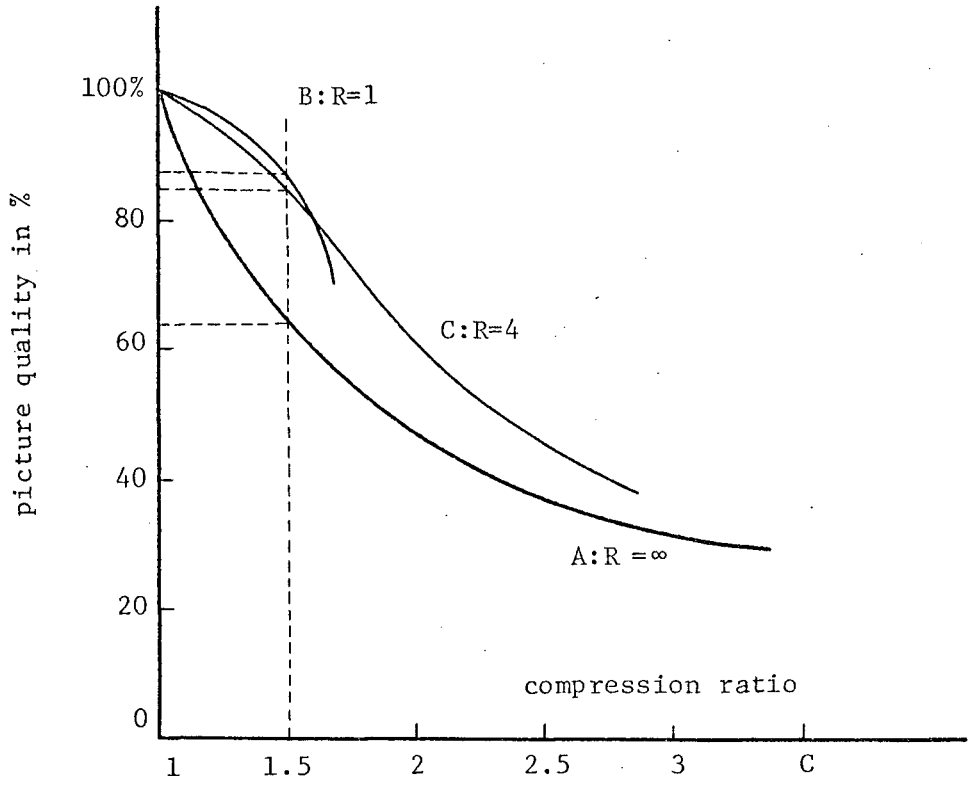

Fig. 3.14 Picture quality vs. compression ratio

A. band limited pictures
B. compressed pictures R=1
C. compressed pictures R=4

Fig. 3.15 Original picture

Fig. 3.16 Output picture corresponds to double-sideband transmission; fx = fm

3.15	3.16
3.17	3.18

Fig. 3.17 Output picture corresponds to single sideband transmission fx = fm

Fig. 3.18 Same as 3.16 except fx = 1/2 fm

this picture is obviously superior to the remaining two. Fig. 3.17 corresponds to a single sideband modulation. Fig. 3.18 is the same as Fig. 3.16 except that fx fm/2. Although figures 3.17 and 3.18 correspond to the same bandwidth in plane P_2 but Fig. 3.18 looks more pleasing than 3.17 in spite of the fact that 3.17 contains higher frequencies and more details can be observed. The noise in Fig. 3.17 due to the brick wall stop, mentioned in section 3.3.2, is another factor contributing to low quality However, single sideband simulation should be used to avoid the complexity of two synchronous chopping wheels for stopping the high spatial frequencies of both sides of the spectrum. It also corresponds to the practical case.

From Fig. 3.14 we see that for a compression ratio smaller than 1.6 the system with OFF:ON ratio R=1 gives a higher output picture quality.

With the same compression ratio, say C = 1.5, Fig. 3.14 shows that for R = 1 the degradation of the picture is about 10%, for R = 4 about 13%, whichmeans with this system we gain about 25% equivalent picture quality over the bandlimited picture with the same bandwidth. For a higher compression ratio, a higher value of R is necessary but the quality of the picture decreases faster as fx is lowered and the advantage over the bandlimited system is very small. This point leads us to the suggestion of attempting to restore the quality of the picture by boosting the high frequencies.

3.7 High Frequency Boost

We can boost the high frequencies to increase the quality of the picture.

The high frequency boost is a high pass filter which cuts down one part of the low frequency range up to about .75 MHz. The results using the high frequency boost are shown in Fig. 3.19, 3.20 and 3.21.

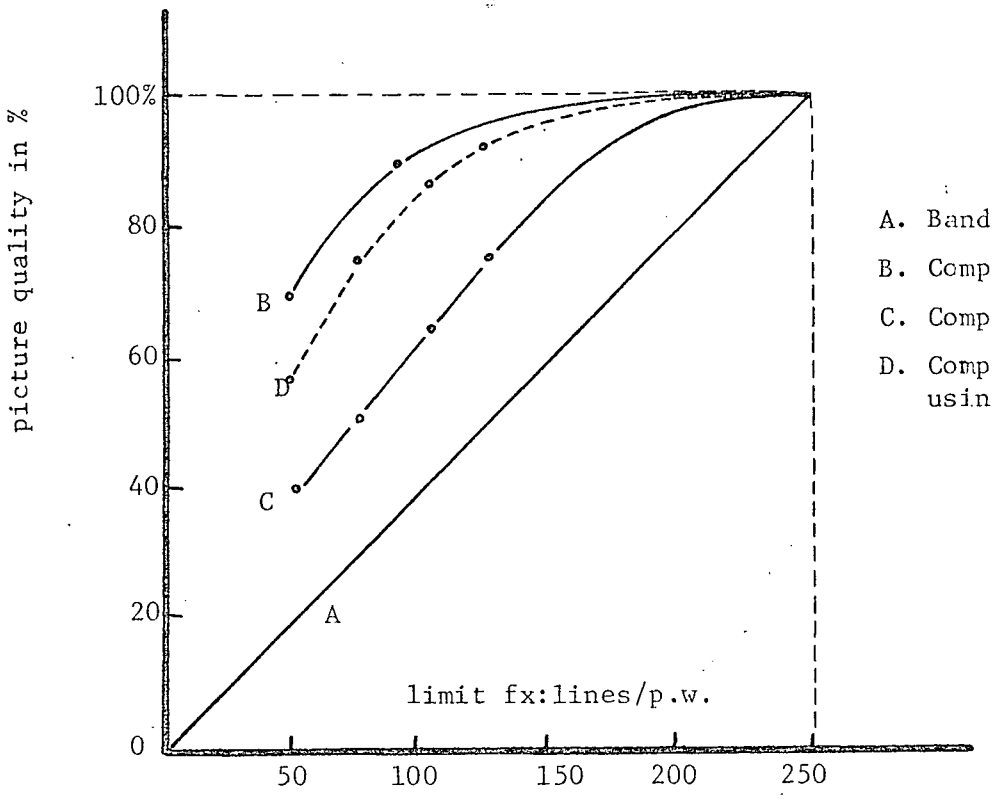

Fig. 3.19 Results of "the high frequency boost"

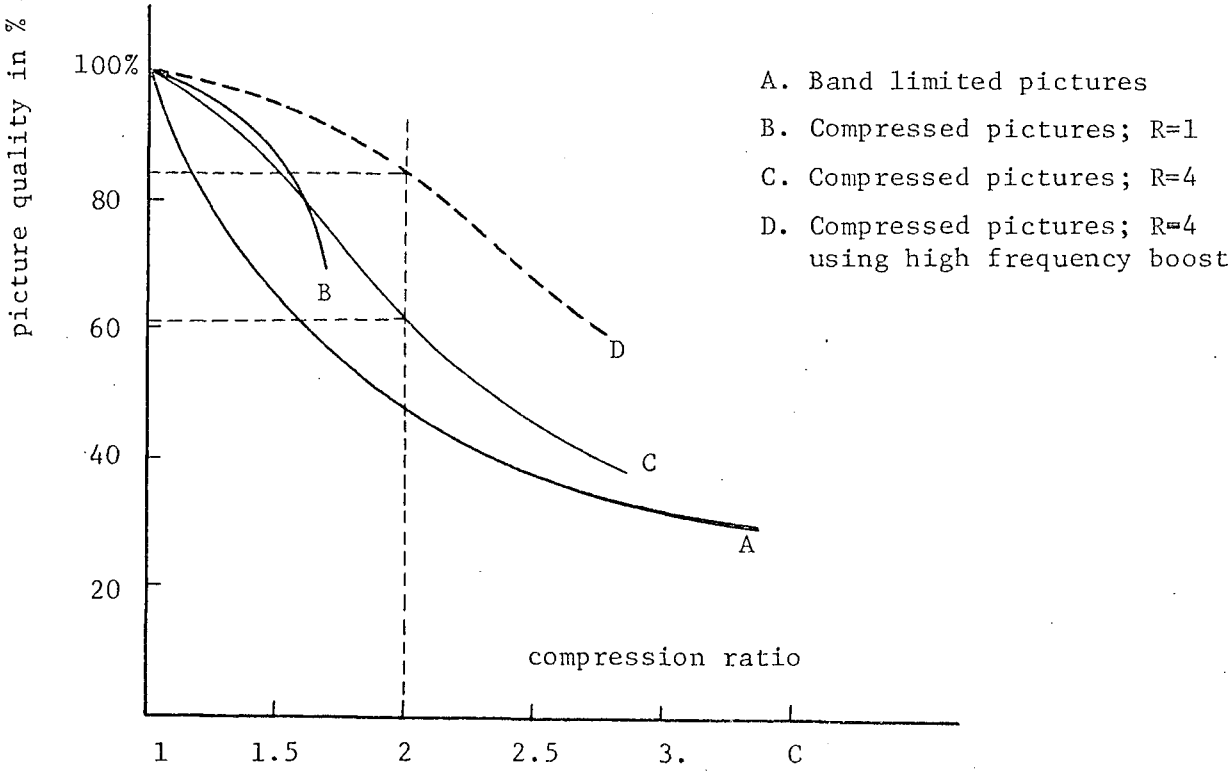

Fig. 3.20 Curves picture-quality vs. compression ratio showing effects of the "high frequency boost"

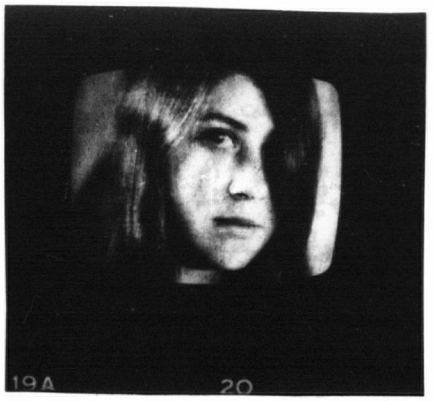

(a)

(b)
C = 1.5

(e)
C = 1.5

(c)
C = 1.8

(f)
C = 1.8

(d)
C = 2.5

(g)
C = 2.5

Fig. 3.21 Effect of the "high-frequency boost"

(a) normal single sideband picture
(b),(c),(d) compressed pictures, R=4, without high frequency boost
(e),(f),(g) compressed pictures, R=4, with high frequency boost

For C > 2 Fig. 3.20 shows that the picture quality increases about 20% when using the high frequency boost with respect to the ordinary compressed picture. Better results still can be expected because of the limitation in this experiment that the h.f. boost is an R.C filter whereas a brick wall filter has been used to limit the quality of the low quality pictures. The two filters should, ideally, have similar slopes on their attenuation skirts.

IV. MOTION PICTURE TEST

It is plausible to expect that motion picture reproduction will enhance some defect in a compression scheme. The purpose of this chapter is to describe experiments used to investigate this problem. It is shown, perhaps surprisingly, that a moving picture can be compressed by a larger amount than a static one before deterioration becomes noticeable.

In place of a test pattern, a projector with 16 mm film is used. The projector speed is adjusted to match the T.V. camera in the sense of avoiding stroboscopic effects. Different types of film were used for testing the flickering effect. It is found that:

(1) No flickering could be perceived when fx > 125 lines/p.w. and the flicker effect was very weak.

(2) The quality of the picture in the film is generally low because of a long exposure time that is employed in the movie camera.

(3) The most noticeable flicker was produced using a film of a still object and this case will be discussed later.

4.1 Analysis of Motion Picture Projector Mechanism

In order to convey the illusion of motion a number of frames, 16 to 24, are projected per second. To eliminate the "smear" effect between two frames a chopping wheel is used to cut-off the light source when frame changes occur. The sequence of film presentation is illustrated schematically in Fig. 4.1

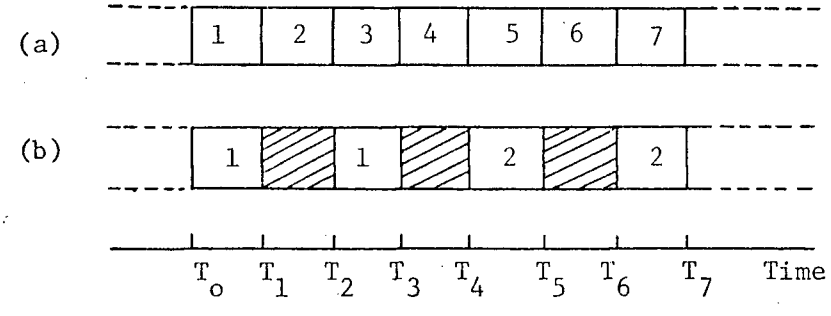

Fig. 4.1 Moving-object film projection

(a) film
(b) sequence of film presentation vs. time

From T_o to T_1 the wheel covers the light source and the frame changing occurs. From T_1 to T_2 the picture is displayed, and so on. If a still object was filmed the projected image vs. time follows the sequence illustrated in Fig. 4.2

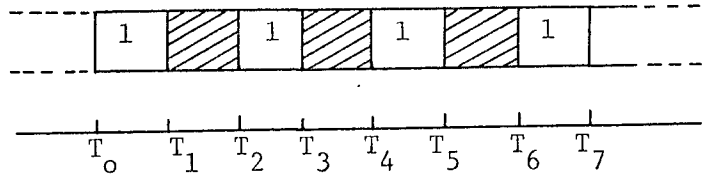

Fig. 4.2 Sequence of a still-object-film presentation

Thus a static picture test and a second chopping wheel in plane P_1 will simulate the moving-picture version of a still object.

The arrangement of apparatus to perform this test is shown in Fig. 4.3.

The speed of the motor driving the chopping wheel can be adjusted to minimize the stroboscopic effect.

4.2 Test Results and Discussion

The same test pattern as Fig. 3.4 was used and the results are presented in Fig. 4.4.

The experimental evidence given in the graph of Fig. 4.4 for a simulated moving picture should be compared with the graph for the same static picture. Contrary to expectation, the static picture presentation is more critical than the moving picture presentation. The action of the picture chopping wheel (Fig. 4.3) seems to make the eye less sensitive to flicker from the chopping wheel in the Fourier transform plane. Thus we

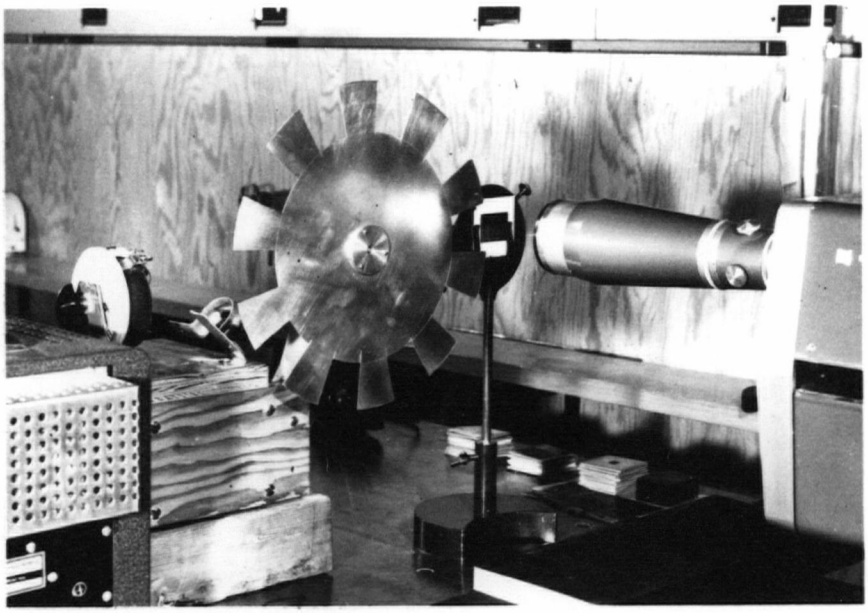

Fig. 4.3 Set up for motion-picture projector simulation

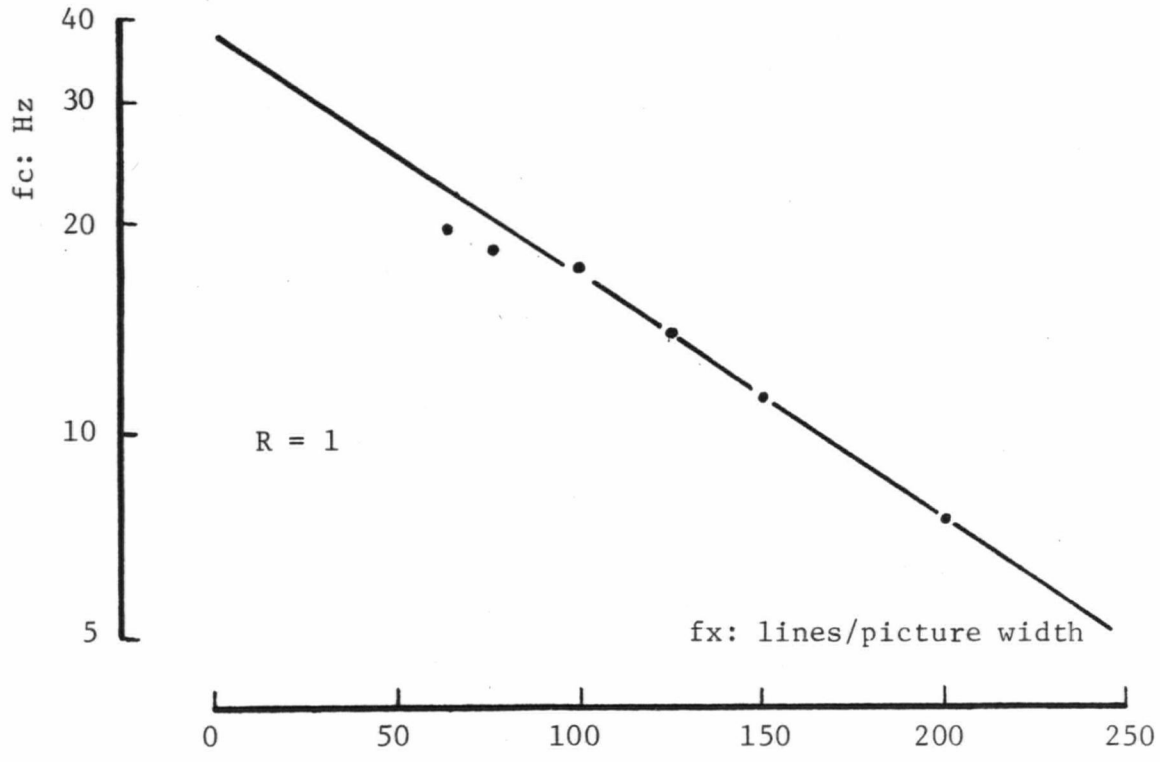

Fig. 4.4 Critical flickering frequency as a function of upper limit spatial frequency fx, for test pattern No. 1, Fig. 3.4, using the apparatus illustrated in Fig. 4.3

can expect more bandwidth compression using a "moving picture" than a static picture.

Small scratches and the slight side way movement in the projector give tremendous changes of the spectrum in Fourier transform plane, and the reconstruction suffers in consequence from pronounced "noise" effects. The same film used with an incandescent illuminator and a normal projector produced only slight noise effects. Good results were obtained using the laser source only with nearly new film.

V. CONCLUSIONS

A scheme for T.V. band compression is described. It is based on the eye's sensitivity to flicker in a sense which is explored in the thesis. The method is supported by psychophysical experiments using a simulated version of the television system.

In Chapter II, an adequate theory has been used to check the design of the simulated television system. In this section the "linearity" of frequency with position in the Fourier transform plane is established.

The major findings of the thesis are contained in Chapter III. There it is shown that the sensitivity of the eye to flicker, fc, is independent of the OFF to ON ratio and this rather surprising result would lead one to expect unlimited compression ratio if the criteria were based solely on the absence of flicker. Experimentally the maximum compression ratio investigated was 2.75:1; at this ratio, however, the reduction of "picture quality" was clearly marked. A high frequency boost was proposed and it is shown that this is effective to a considerable degree in arresting the fall off in quality with increase of C. In order to measure picture quality, a comparison technique was proposed in which a compressed picture was "matched" to a normally scanned band-limited picture. The results using this technique are contained in the important graphs, Fig. 3.20.

It is shown in Chapter IV that the motion-picture case is less critical than the static picture case and that one can expect more bandwidth reduction for the moving picture transmission than for the static picture one.

Some disadvantages remain in the simulation system:

(1) Noise due to coherent light source. "Contour noise" makes the critical flicker frequency higher than it should be.

(2) The brick wall filter used in the Fourier transform plane did not match the R-C high frequency-boost circuit. Some improvement might be expected if such a match was made.

The band compression scheme proposed here depends upon the properties of the eye. It seems reasonable to suggest, for further work, that it be used along with a purely statistical encoder such as the run-length encoder of Cherry et al.

REFERENCES

1. M. P. Beddoes and Otto Meier, "Flicker Effect and Television Compression", IEEE Transactions on Information Theory, volume IT16, No. 2, pp. 214-218, March, 1970.

2. Otto Meier, "Television Picture Transmission and Optical Signal Processing", M.A.Sc. Thesis, Dept. of Electrical Engineering, U.B.C., July, 1968.

3. T. S. Huang and O. J. Tretiak, "Research in Picture Processing", Optical and Electro-Optical Information, MIT press, 1965; pp. 45-57.

4. Colin Cherry et al., "An Experimental Study of the Possible Bandwidth Compression of Visual Image Signals", Proceedings of the IEEE, vol. 51, No. 11; pp. 1506-1517, November, 1963.

5. W. F. Schreiber, "Picture Coding", Proceedings of the IEEE, vol. 55, No. 3, pp. 320-330, March, 1967.

6. A. Vander Lugt, "Operational Notation for the Analysis and Synthesis of Optical Data-Processing Systems", Proceedings of the IEEE, vol. 54, No. 8, pp. 1055-1063, August, 1966.

7. J. W. Goodman, "Introduction to Fourier Optics", McGraw-Hill, 1968.

8. Anthanasios Papoulis, "System and Transforms with Applications in Optics", McGraw-Hill, 1968.

9. M. Abramowitz and I. A. Stegun, "Handbook of Mathematical Functions", New York:Dover, 1964; p. 304.

10. Brian J. Thompson and John B. Develis, "Introduction to Coherent Optics and Holography", Paper 680012 presented at SAE Automotive Engineering Congress, Detroit, January 1968.

11. Pratt, W. K., "A Bibliography on Television Bandwidth Reduction Studies", IEEE Transactions on Information Theory, vol. IT-13, No. 1, pp. 114-115, January, 1967.

APPENDIX

A-1 Properties of Function ψ

For the convenience of the reader some properties of ψ functions from Vander Lugt's paper [6] are given here.

Definition of function ψ .

$$\psi(x,y;f) \equiv \exp[j \frac{kf}{2}(x^2 + y^2)]$$

The properties of ψ function:

P-i $\quad \psi(x,y;f) = \bar{\psi}(x,y;-f)$

P-ii $\quad \psi(-x,-y;f) = \psi(x,y;f)$

P-iii $\quad \psi(x,y;f_1)\ \psi\ (x,y;f_2) = \psi(x,y;\ f_1 + f_2)$

P-iv $\quad \psi(x,y;f_1)\ \bar{\psi}\ (x,y;f_2) = \psi(x,y;f_1 - f_2)$

$$= \bar{\psi}\ (x,y;\ f_2 - f_1)$$

P-v $\quad \psi(cx,cy;f) = \psi(x,y;\ c^2 f)$

P-vi $\quad \bar{\psi}(x;f_1)\ \bar{\psi}\ (x,y;f_2) = \bar{\psi}(y;f_2)\ \bar{\psi}\ (x;f_1 + f_2)$

P-vii $\quad \bar{\psi}(y;f_1)\ \bar{\psi}\ (x,y;f_2) = \bar{\psi}(x;f_2)\ \bar{\psi}(y;f_1 + f_2)$

P-viii $\quad \psi(x-u,y-v;f) = \psi(x,y;f)\ \psi\ (u,v;f)\ \exp[-jkf(ux + vy)]$

P-ix $\quad \psi(x,y;f) = \psi(x,f)\ \psi\ (y;f)$

P-x $\quad \lim_{d \to 0} \bar{\psi}(x,y;d) = 1$

P-xi $\quad \lim_{d \to \infty} d\psi(x,y;d) = \delta(x,y)$

A-2 Proof of Equations 2.3, 2.5, 2.7

The optical system and block diagram to obtain Fourier transform in plane P_2 is shown in Fig. A.2.1.

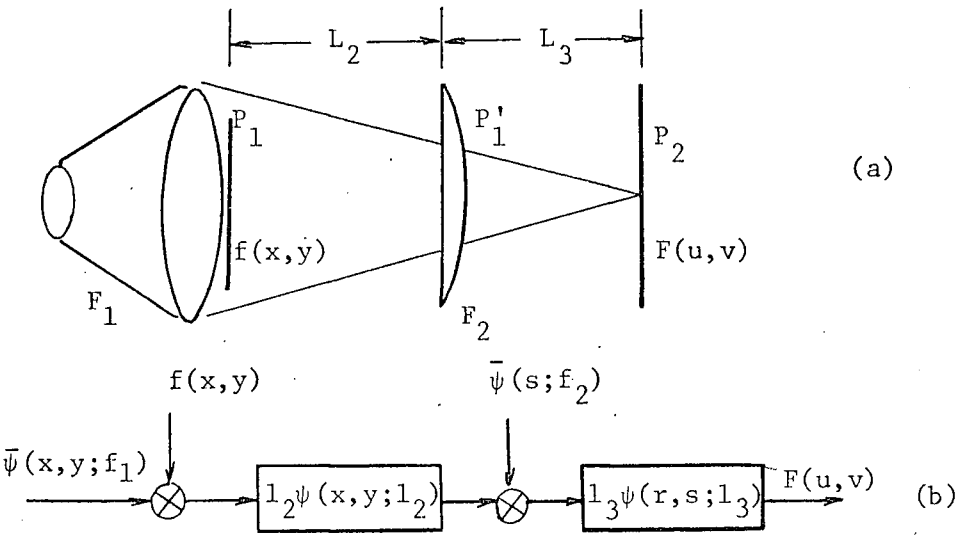

Fig. A.2.1 One-dimensional Fourier Transform Optical System

(a) Optical System
(b) Block diagram

From the block diagram we get

$$F(u,v) = l_2 l_3 \iint_{P_1}\iint_{P_1'} \bar{\psi}(x,y;f_1) f(x,y) \psi(x,y;l_2) \psi(r,s;l_2) \exp[-jkl_2(rx + sy)] \bar{\psi}(s;f_2) \psi(r,s;l_3) \psi(u,v;l_3) \exp[-jkl_3(ur + vs)]\, dxdy\, drds \tag{A.2.1}$$

After using P-iii F(u,v) becomes

$$F(u,v) = l_2 l_3 \psi(u,v;l_3) \iint_{P_1}\iint_{P_1'} \psi(x,y;l_2 - f_1) f(x,y) \psi(r,s;l_2 + l_3) \bar{\psi}(s;f_2) \exp[-jkl_2(rx + sy)] \exp[-jkl_3(ur + vs)]\, dxdy\, drds \tag{A.2.2}$$

Using P-vi

$$f(u,v) = l_2 l_3 \psi(u,v;l_3 \iint_{P_1} \iint_{P_1'} \psi(x,y;l_2-f_1) f(x,y) \psi(r;l_2 + l_3)$$
$$\psi(s;l_2 + l_3 - f_2) \exp\left[-jkl_2 r\left(x + \frac{l_3}{l_2} u\right)\right]$$
$$\exp\left[-jkl_2 s\left(y + \frac{l_3}{l_2} v\right)\right] dxdy\, drds$$

From Handbook of Mathematical Functions, M. Abramowitz and I. A. Stegun [9], we have the relation (A.2.4)

$$\iint_{-\infty}^{\infty} \psi(x,y;f_1) \exp[-jkf_2(rx + sy)]\, dxdy = \frac{C}{f_1} \psi(r,s;f_2^2/f_1) \qquad (A.2.4)$$

Using relation A.2.4 to carry out r,s integration

$$F(u,v) = C \cdot \psi(u,v;l_3) \iint_{P_1} \psi(x,y;l_2-f_1)\, f(x,y) \bar{\psi}\left[x + \frac{l_3}{l_2} u;\ \frac{l_2^2}{l_2 + l_3}\right]$$
$$\bar{\psi}\left[y + \frac{l_3}{l_2} v;\ \frac{l_2^2}{l_2+l_3-f_2}\right] dxdy \qquad (A.2.5)$$

This is equation 2.3. in Chapter II.

Imaging condition

To perform the imaging system we use property P-xi to get the position of lenses. By property P-xi,

$$\frac{l_2^2}{l_2+l_3-f_2} \bar{\psi}\left[y + \frac{l_3}{l_2} v;\ \frac{l_2^2}{l_2+l_3-f_2}\right] = \delta\left(y + \frac{l_3}{l_2} v\right) \qquad (A.2.6)$$

A.2.6 will be satisfied when

$$\frac{l_2^2}{l_2+l_3-f_2} \to \infty \quad \text{or} \quad l_2 + l_3 = f_2$$

$$\frac{1}{L_2} + \frac{1}{L_3} = \frac{1}{F_2} \qquad (A.2.7)$$

This is equation 5 in Chapter II.

Fourier transform condition

Applied equation A.2.6 in A.2.5 and using the sifting property of the δ function, we have:

$$F(u,v) = C\cdot\psi(u,v;l_3)\cdot\psi\left(\frac{l_3}{l_2}v;\ l_2-f_1\right)\int \psi(x;l_2-f_1)f(x)-\frac{l_3}{l_2}v)\ \bar{\psi}\left[x+\frac{l_3}{l_2}u;\ \frac{l_2^2}{l_2+l_3}\right]\,dx$$

Using property P-viii and collecting terms, we have:

$$F(u,v) = C\cdot\ (u;l_3)\left[(v;l_3 + (l_2-f_1)\frac{l_3^2}{l_2^2}\right]\int f(x,-\frac{l_3}{l_2}v)\ [x;l_2-f_1-\frac{l_2^2}{l_2+l_3}\ ]\ \exp\left[-jk\left(\frac{l_2l_3}{l_2+l_3}\right)xv\right]\,dx \qquad (A.2.9)$$

A.2.9 has almost a Fourier transform form. We will use P-x to make the ψ function inside the integral be equal to unity.

Thus by P-x

$$l_2 - f_1 - \frac{l_2^2}{l_2+l_3} = 0 \qquad (A.2.10)$$

or

$$L_2 + L_3 = F_1 \qquad (A.2.11)$$

This is equation 2.7 in Chapter II and F(u,v) now is:

$$F(u,v) = C\cdot\psi(u,l_3)\psi\left[v;l_3 + (l_2-f_1)\frac{l_3^2}{l_2^2}\right]\int f(x,-\frac{l_3}{l_2}v)\exp\left[-jk\left(\frac{l_2l_3}{l_2+l_3}\right)xv\right]\,dx \qquad (A.2.12)$$

This equation shows that in plane P_2 we obtain a one-dimensional Fourier transform F(u,v) of f(x,y).